JTTEE5 9:100-106

Development of Coating Structure and Adhesion During High Velocity Oxygen-Fuel Spraying of WC-Co Powder on a Copper Substrate

V.V. Sobolev, J.M. Guilemany, and J.A. Calero

(Submitted 17 October 1997; in revised form 5 December 1999)

This paper deals with the mathematical modeling of the development of the WC-Co coating structure and adhesion on a copper substrate during high velocity oxygen-fuel (HVOF) spraying. Two types of substrates are considered: smooth (polished) and rough (grit blasted). Variations of solidification time, solidification velocity, thermal gradient, and cooling velocity in the coating and substrate interfacial region are studied. Development of the amorphous and crystalline structures in the coating and of the crystalline structure in the substrate interfacial region is discussed. Behavior of the crystal size and intercrystalline distance with respect to the thermal spray parameters and morphology of the substrate surface is analyzed. Optimal conditions for the formation of fine and dense crystalline structure are determined. Structural changes in the solid state of the substrate occurring because of heating and rapid cooling are considered. Mechanical and thermal mechanisms of development of the substrate-coating adhesion are discussed. Results obtained agree well with experimental data.

Keywords HVOF spraying, structure formation, modeling, WC-Co coating, copper substrate

1. Introduction

Coating structure developed during solidification plays an important role in formation of the coating properties.[1, 2] It depends on the heat transfer processes in the coating and substrate.[1–6]

This paper studies development of the coating structure and the substrate-coating adhesion during high velocity oxygen-fuel (HVOF) spraying of WC-Co powder onto a copper substrate. The investigation is a mathematical modeling based on the model developed in[7] and on the results of the heat transfer analysis undertaken in[5]. Two types of substrate surfaces are considered: smooth (polished) and rough (grit blasted). Special attention is given to structure formation in the first coating layer and the substrate interfacial region where the substrate-coating adhesion and bonds are formed. Different mechanisms of the adhesion development are discussed. The results agree well with the experimental data. They also can be used in the analysis of coating defects, such as porosity, chemical nonhomogeneity, and residual stresses, by the methods developed in [8-12].

In the basic version of the mathematical simulation, the following parameters were taken.[5] The thickness of the substrate zone involved in the coating-substrate heat transfer is 3 mm. The coating layer thickness, δ, is 15 μm. The substrate initial temperature, T_{10}, is 20 °C. Using the modeling results obtained in[5] and their correlations with the experimental data on analysis of the substrate-coating interface,[15] the following values of the heat transfer coefficients were estimated. The heat transfer coefficient at the upper surface of a coating layer, α, was taken to be 1000 W m^{-2} K^{-1}. The contact heat transfer coefficient at the substrate coating interface, α_c, for the smooth substrate surface was $6.67 \cdot 10^6$ W m^{-2} K^{-1} and for the grit-blasted substrate surface $\alpha_c = 3.33 \cdot 10^6$ W m^{-2} K^{-1}. The fluid temperature near a coating layer upper surface is 500 °C. The time between application of different coating layers is 1.32 s.[5]

V.V. Sobolev, J.M. Guilemany, and **J.A. Calero,** Thermal Spray Centre, Materials Engineering, Departamento de Ingenieria Quimica y Metalurgia, Universidad de Barcelona, 08028 Barcelona, Spain.

2. Coating First Layer

2.1 Solidification Isotherms

The main heat removal from the first coating layer takes place to the substrate, which is a massive heat sink. Hence, layer solidification occurs first at the substrate-coating interface and continues in the direction of the layer upper surface.[5] Because of cooling of the upper layer surface by the surrounding gases, an additional solidification front appears, moving toward the interface. But this solidification process is negligible in comparison with that starting at the interface.[5] The latter solidification process becomes even more pronounced in the case of the copper substrate because of the good thermal properties of copper.

During motion of the WC-Co powder particles at the spray distance, tungsten carbide dissolution occurs and a Co-W-C alloy system is formed. Alloy solidification depends essentially on movement of the surfaces having the liquidus temperature and solidus temperature, which bound the solid-liquid (mushy) zone region. Behavior of liquidus and solidus isotherms follows a similar pattern. Here, behavior at the solidus is discussed.

The movement of this isothermal surface is characterized by a velocity of this movement (solidification velocity) v_{S2}, thermal gradient G_{S2}, and cooling velocity v_{CS2} (which is a product of v_{S2}

and G_{S2}: $v_{CS2} = v_{S2} \cdot G_{S2}$) at this surface. The solidus isotherm moves with the velocity, v_{S2}, at first rapidly and then more slowly because of the latent heat extraction. The thermal gradient at the solidus, G_{S2}, is steep near the substrate-coating interface. Then it decreases, at first rapidly and later more slowly as the heat removal becomes competitive with extraction of the latent heat of solidification. The cooling velocity, v_{CS2}, at the solidus isotherm (which is a product of v_{S2} and G_{S2}) decreases sharply in the vicinity of the interface and then varies more slowly.

Mean values of v_{S2}, G_{S2}, and v_{CS2} were also calculated with respect to time as the integral mean values during the solidification process. Mean solidification velocity varies nonuniformly with increasing initial temperatures of substrate and coating for both smooth and rough substrate surfaces (Fig. 1). The surface roughness causes an increase in the maximum values of v_{S2} with respect to layer (coating) initial temperature, T_{20}, due to an increase in the thermal gradients between the layer and the substrate. A further increase in T_{20} causes an increase in the heat content of the layer and hence the mean value of v_{S2} starts to decrease after achieving the maximum value. In the case of the grit-blasted surface, this occurs at higher values of T_{20} than for the smooth substrate surface because the surface roughness contributes to slowing down of the heat transfer between the layer and the substrate. This slowing down also explains a decrease in the mean value of v_{S2} with respect to substrate initial temperature in the case of the grit-blasted substrate surface.

With an increase in T_{10}, melting of the substrate interfacial region occurs earlier. Because of latent heat absorption, this melting causes an increase in the mean value of G_{S2} (Fig. 2). With a further increase in T_{10}, a difference in temperatures between the layer and the substrate decreases and the role of the substrate as a heat sink also decreases. Both these factors contribute to a decrease in the mean value of G_{S2}. Their influence on the behavior of G_{S2} manifests itself in a sharp slowing down of an increase in G_{S2} with respect to T_{10}. With the grit-blasted surface of the substrate, the above factors leading to a decrease in the mean value of G_{S2} are dominant and this value decreases as T_{10} increases (Fig. 2).

Fig. 2 also shows that an increase in the layer initial temperature, T_{20}, generally gives rise to the mean value of G_{S2}. For the smooth surface in the range of T_{20} from 1485 to 1490 °C, this mean value slightly decreases with an increase in T_{20} due to acceleration in the layer solidification and more rapid removal of the extracted latent heat to the substrate.

The mean value of the cooling velocity v_{CS2} increases as T_{20} increases and exhibits the nonuniform behavior with respect to T_{10} (Fig. 3). Mean values of v_{S2}, G_{S2}, and v_{CS2} decrease with an increase in the layer thickness.

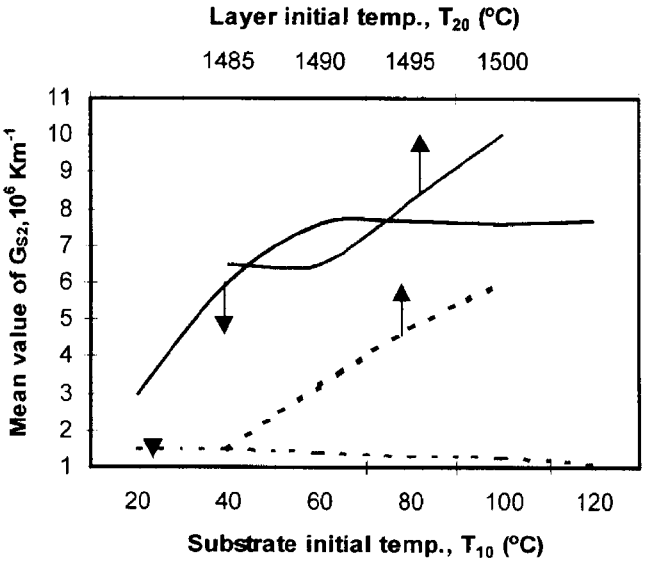

Fig. 2 Variation of mean values of the thermal gradient, G_{S2}, with respect to initial temperatures of substrate and layer for smooth (continuous lines) and rough (discontinuous lines) surfaces.

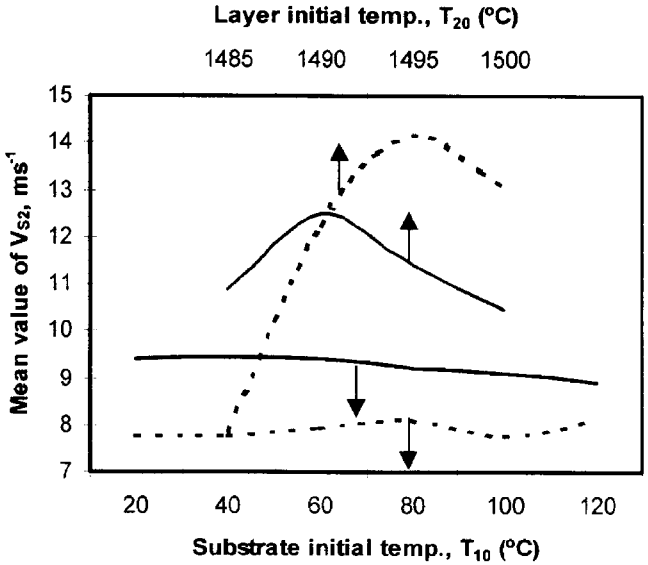

Fig. 1 Variation of mean values of the solidification velocity, v_{S2}, with respect to initial temperatures of substrate and layer for smooth (continuous lines) and rough (discontinuous lines) surfaces.

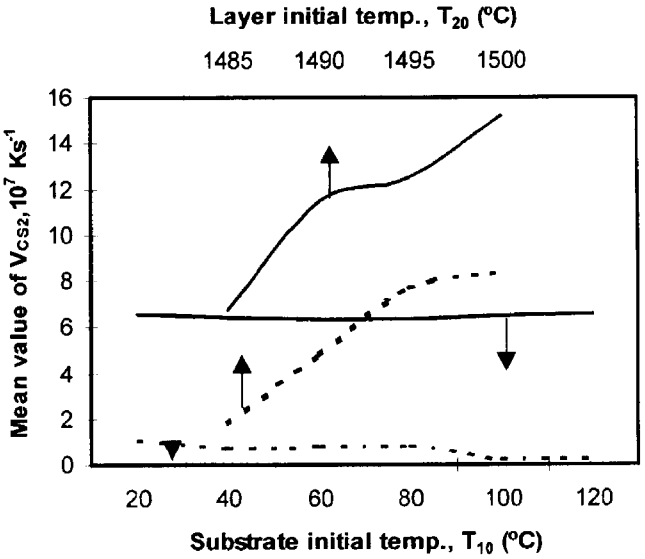

Fig. 3 Variation of mean values of the cooling velocity, v_{CS2}, with respect to initial temperatures of substrate and layer for smooth (continuous lines) and rough (discontinuous lines) surfaces

2.2 Structure Formation

In the first layer of the coating and in subsequent layers, both amorphous and crystalline structures may be formed due to very high cooling velocities. Earlier, it was shown that the alloy phase of the WC-Co coating sprayed on a low carbon steel substrate had a high glass forming ability and, hence, a high probability of developing an amorphous structure.[7] This probability was confirmed by coating characterization.[13] The WC-Co coating structures on the aluminum alloy substrate and on the copper substrate are similar to that on the steel substrate.[14, 15]

Due to heat transfer from the impinging droplets, the previously developed coating layers can be reheated, and when the temperature reaches 0.4 to 0.6 of the liquidus temperature of the coating alloy, the amorphous structure of the coating can be partially destroyed and transformed to a crystalline one during the time period significantly greater than the characteristic time of the coating solidification.[16] These temperatures can be achieved in the spraying process.[5, 7]

The fine crystalline structure of the layer is characterized by ξ, the size of crystals, and η, the distance between them. The values of ξ and η can be calculated using the determined velocities of solidification and cooling and the thermal gradients at the liquidus and solidus isotherms. The following formulas for ξ and η are used:[17]

$$\xi = a v_{S2^b} G_{S2^C} \quad \text{(Eq 1)}$$

$$\eta = d v_{CS2^e} \quad \text{(Eq 2)}$$

For calculating the coating layer structure, the following parameters in Eq 1 and 2 were used: $a = 10^{-4}$, $b = -0.25$, $c = -0.5$, $d = 3.8$, and $e = -0.4$.

The mean values of ξ for the smooth substrate surface vary nonuniformly with an increase in T_{10} and they decrease as T_{20} increases (Fig. 4). Fig. 4 shows that in the case of the grit-blasted surface, the mean values of ξ exhibit nonuniform behavior with respect to T_{10} and T_{20}. The mean values of η_{S2} vary nonuniformly with an increase in T_{10} and T_{20}, both for the smooth and grit-blasted surfaces (Fig. 5). An increase in the layer thickness causes an increase in the mean values of ξ and η_{S2} (Fig. 6).

The minimum values of ξ, corresponding to the finest crystalline structure in the case of the smooth substrate surface, are expected when T_{10} = 70 to 120 °C, T_{20} = 1495 to 1500 °C, and δ = 5 to 10 μm. In the case of the grit-blasted surface, the finest crystalline structure is likely to occur when T_{10} = 20 to 50 °C and T_{20} = 1495 °C.

The densest crystalline structure seems to take place when η is at its minimum. For the smooth substrate surface, it is predicted to be formed if T_{10} = 120 °C, T_{20} = 1495 to 1500 °C, and δ = 5 to

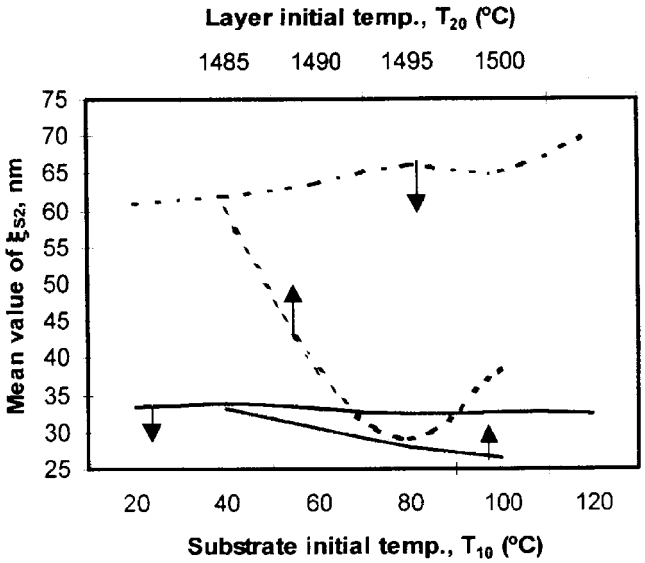

Fig. 4 Variation of mean values of the crystal size, ξ_{S2}, with respect to initial temperatures of substrate and layer for smooth (continuous lines) and rough (discontinuous lines) surfaces.

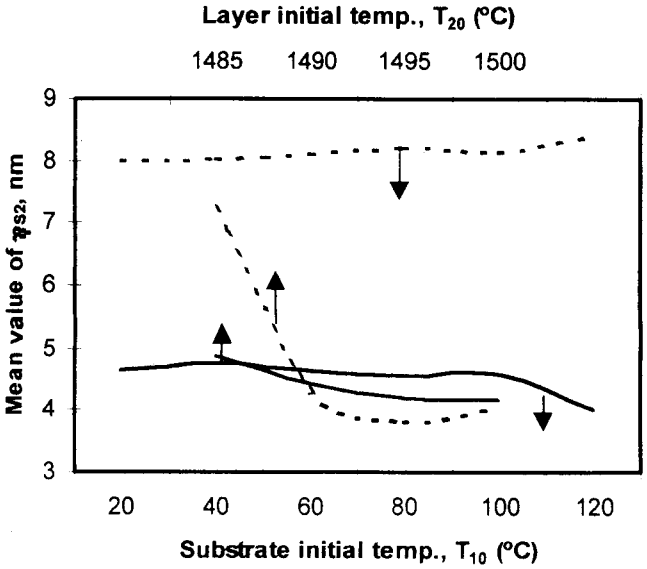

Fig. 5 Variation of mean values of the intercrystalline distance, η_{S2}, with respect to initial temperatures of substrate and layer for smooth (continuous lines) and rough (discontinuous lines) surfaces.

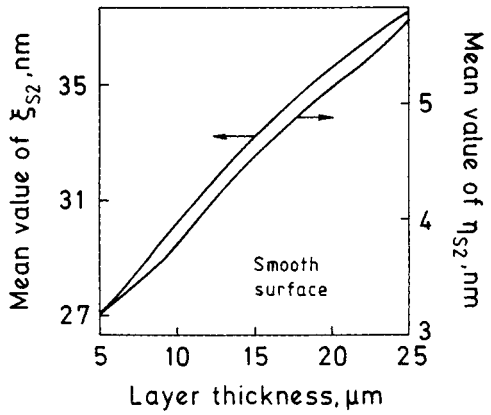

Fig. 6 Variation of mean values of the crystal size, ξ_{S2}, and intercrystalline distance, η_{S2}, with respect to the layer thickness for the smooth surface.

10 μm. In the case of the grit-blasted surface, the densest structure is likely to be when T_{10} = 20 to 50 °C and T_{20} = 1495 °C.

3. Substrate Interfacial Region

3.1 Solidification Isotherms

Heat transfer from the coating causes an increase in the temperature in the substrate interfacial region up to the melting point. Melting velocities characterized by movement of the liquidus and solidus isothermal surfaces increase near the interface.

After melting and attaining the maximum melting depth, solidification starts, and the velocities of the liquidus and solidus isotherms enhance in the vicinity of the substrate-coating interface. This increase is slower than that of the melting velocities due to the latent heat extraction.

The thermal gradients at the liquidus and solidus isothermal surfaces decrease during melting and continue to decrease during solidification, approaching the interface. The cooling velocity increases in the interface direction, and near the interface, it experiences a sharp increase because of a decrease in the latent heat extraction, which becomes less than the heat removed by the substrate.

The mean values of the solidification velocity (velocity of the solidus isotherm), thermal gradient at the solidus, and cooling velocity decrease with an increase in the layer thickness and initial temperatures of the substrate and the layer. The above parameters of solidification in the substrate interfacial region enable calculation of the characteristics of the crystalline structure developed.

3.2 Development of Crystalline Structure

Crystal size ξ in the substrate interfacial region is found from Eq 1, and intercrystalline distance η is determined from the equation[17]

$$\eta = f \bullet G^{-g} \qquad \text{(Eq 3)}$$

The parameters are set to $a = 3 \bullet 10^{-4}$, $b = -0.25$, and $c = -0.5$ in Eq 1 and $f = 0.88$ and $g = 0.275$ in[7].

Modeling indicates that the crystal size, ξ, decreases in the direction of the interior of the substrate. The intercrystalline distance, η, also decreases in the same direction.

For the smooth substrate surface, the mean values of ξ and η grow with the initial temperatures of the layer and substrate because of a decrease in the velocities of solidification and cooling and thermal gradients (Fig. 7). In this case, the mean crystal size and intercrystalline distance practically do not vary with the increasing layer thickness.

In the case of the grit-blasted surface, the mean values of ξ and η vary nonuniformly with respect to T_{10} and δ (Fig. 8 and 9). They also exhibit nonuniform behavior with respect to T_{20}, attaining the minimum values at T_{20} = 1490 °C.

The minimum values of ξ and η corresponding to the finest and densest crystalline structures, respectively, in the substrate interfacial region in the case of the smooth surface occur when T_{10} = 20 to 50 °C and T_{20} = 1482 to 1485 °C. In the case of the grit-blasted surface, the minimum ξ and η are when T_{10} = 90 to 100 °C, T_{20} = 1490 °C, and δ = 5 to 10 μm.

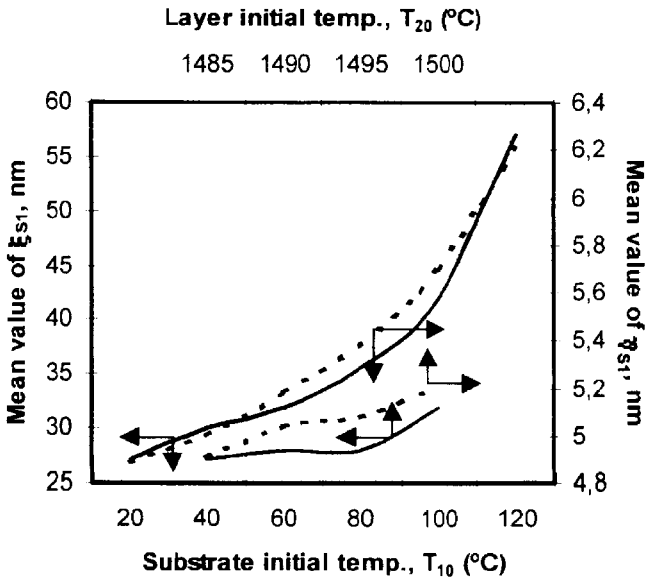

Fig. 7 Variation of mean values of the crystal size, ξ_{S1} (continuous lines), and intercrystalline distance, η_{S1} (discontinuous lines), with respect to initial temperatures of substrate and layer for the smooth surface.

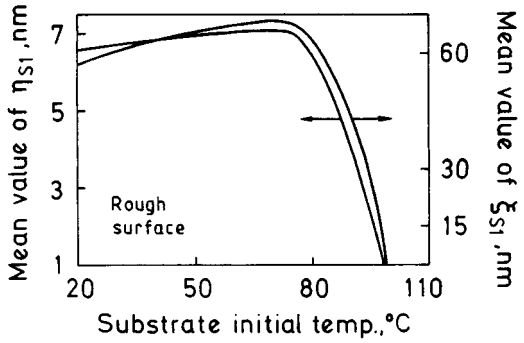

Fig. 8 Variation of mean values of the crystal size, ξ_{S1}, and intercrystalline distance, η_{S1}, with respect to substrate initial temperatures for the grit-blasted surface.

3.3 Structural Changes in the Solid State

Structural changes in the solid state of the substrate can occur because of heating and rapid cooling. Such changes were found in steel and aluminum alloy substrates coated with the WC-Co HVOF sprayed coatings.[13, 14]

In the case of the copper substrate, the grit blasting gave a deformed zone, which was much greater in depth than that in the steel and the aluminum alloy substrates. These differences can be caused by differences in the work hardening characteristics of the materials. The thermal pulses from the initial splats are then sufficient for partial recrystallization of the copper. But the temperature-time characteristics of the heat transfer are insufficient to eliminate the relatively stable structures of the shear bands developed due to the energy input from the roughening. As a process result, near the substrate-coating interface, the micro-

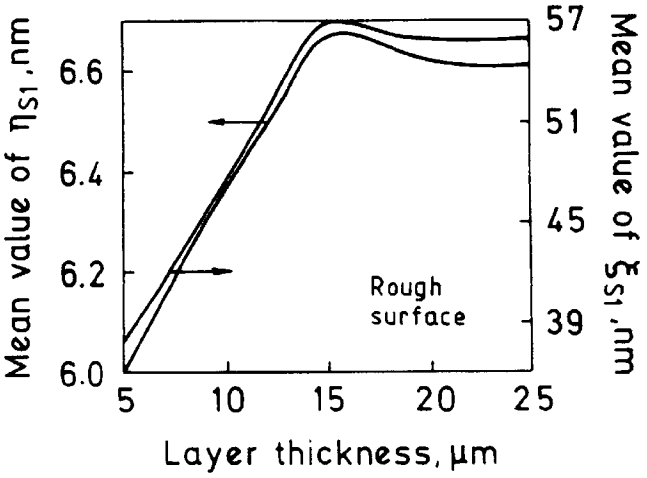

Fig. 9 Variation of mean values of the crystal size, ξ_{S1}, and intercrystalline distance, η_{S1}, with respect to layer thickness for the grit-blasted surface

structural characteristics are similar to those formed when melting and rapid solidification of copper occur. The modeling results show that the maximum temperature at 5 to 10 μm below the interface surface is 925 to 825 °C, which is markedly below the copper melting point.

The heat transfer from the initial splats produced recrystallization and recovery to a depth of about 40 μm, the limit of the plastically deformed region. The modeling results indicate that at this depth from the interface the maximum temperature was between 550 and 600 °C, which is sufficient to produce the above effects.

In the case of the smooth (polished) copper surface, the heat transfer from the initial splats was sufficient to melt the copper in the immediate vicinity of the interface, but insufficient to develop a melted zone over the entire interfacial region. The polished substrate was free from cold work and, therefore, copper recrystallization was not expected to occur below the melted zone. The thermal energy from the initial splats was not sufficient to increase the grain size or cause any other microstructural changes in the substrate.

For both the polished and grit-blasted substrates, the modeling results show that the heat transfer from the second and subsequent layers of the coating does not cause any changes in the substrate material.

4. Coating Layers of an Initial Deposition

In the deposition process of the initial coating layers, the distance between them and the substrate increases and the solidification of these layers is slower than that of the first layer.[5] Therefore, the crystalline parameters ξ and η are increased. They vary with T_{10}, T_{20}, δ, and the substrate surface morphology in the same manner discussed for the first layer of the coating (Fig. 4 to 9).

5. Coating-Substrate Adhesion

The adhesion of thermally sprayed coatings is greatly influenced by mechanical and thermal interaction between the coating and the substrate as well as by the microstructures developed at the interfacial region. For this reason, much effort has been applied to the analysis of these phenomena.[5–7, 13, 14]

To obtain good adhesion, it is necessary to have close contact between the substrate and the coating first layer. Great pressures are developed during flattening of an impinging droplet on the substrate surface.[6, 18] The pressure, P, generated upon impact due to the kinetic energy of the droplet is maximum in the central part of a splat, where it is 10^3 to 10^4 times the atmospheric pressure.[6, 18] Then, the value of P decreases toward the splat periphery. An increase in the kinetic energy of the droplet causes an increase in the pressure P and causes the pressure variation along the splat to be more severe.[18]

Close contact between the substrate and the coating can be obtained when the pressure developed, P, exceeds the capillary presure, P_σ, which arises at the substrate-coating interface because of the roughness. Thus, a ratio $\zeta = P/P_\sigma$ could be correlated with the substrate-coating microadhesion. The results obtained in[18] show that the ratio ζ (and hence microadhesion) increases with an increase in the density, viscosity, and velocity of the impinging droplet and the roughness of the substrate surface. The value of ζ decreases with an increase in the droplet mass loss upon impact and the surface tension at the substrate-droplet interface. The ratio ζ is maximum in the central part of the splat and decreases in the direction of its periphery. These tendencies correspond to those found experimentally for the substrate-coating microadhesion during thermal spraying.[4]

The generation of great pressures upon the droplet impact and the substrate roughness enable "keying," which is usually assumed to be developed between the coating and the substrate. The results on the substrate-coating thermal interaction obtained in Refs 5 and 7 establish an additional formation mechanism for the substrate-coating microadhesion.

Partial or complete melting in the substrate interfacial zone contributes to development of close contact between the coating and the substrate, and this contact depends essentially on the morphology of the substrate surface. The surface roughness hinders the flow of the flattening droplets on the substrate surface.[19] A greater local heat source is then available from the splat to melt the substrate. This is particularly important for the splat periphery, where the pressure P is not high enough to develop good bonding between the coating and the substrate. The melted substrate interfacial zone can then bond readily to the coating. In the present experiments, the melted region has a depth of about 0.5 μm and good adhesion is obtained.

With the polished surface, the splat spreads over a greater area and, therefore, the heat flux from the splat to the substrate is less and the maximum depth of the melted interfacial region is found to be only about 0.1 μm.

6. Comparison with the Experimental Data

The HVOF spraying was provided with the Plasma Technik AG PT100 system at the Centre of Thermal Spraying, the University of Barcelona. A commercial WC-Co powder was sprayed onto a copper substrate.

The coating microstructure is similar to that described in[13]. The microstructure of the substrate interfacial region depends essentially on the morphology of the substrate surface[15] and

differs markedly from that with the same coating on a steel and an aluminum alloy substrates.[13, 14]

6.1 Substrate-Coating Interfacial Region without Grit Blasting

In the substrate interfacial region, fine crystals were found in the copper, extending for a depth of about 0.1 μm, but in some regions, these crystals were absent. The grain size of the fine copper crystals was 5-20 nm, and a sharp boundary between the fine crystalline structure and original coarse-grained structure of the substrate was observed (Fig. 10a).

The fine crystalline structure develops because of melting of the copper by the heat flux from the first coating layer and its further solidification under very high cooling velocities. No structural changes that could be associated with a heat-affected zone were detected below the fine crystal zone.

The experimental data are consistent with the modeling results, which indicate that the depth of partial melting in the substrate interfacial region is about 0.1 μm[15] and the crystal size is within the experimentally observed range (Fig. 7).

6.2 Substrate-Coating Interfacial Region with Grit Blasting

Four zones were identified in the substrate interfacial region in the case of the grit-blasted substrate surface. Zone 1 was in the substrate immediately adjacent to the interface and consisted of fine 50 nm crystals, making it somewhat larger than that of the polished substrate. The depth of this zone was about 0.5 μm (Fig. 10b). Zone 1 is the region where the copper has been molten. It is consistent with the modeling results, which show that the depth of this zone is about 0.5 μm[5] and the crystal size is about 40 to 60 nm (Fig. 8). The comparison of Fig. 7 and 8 indicates that with the grit-blasted surface, the crystal size is larger than that in the case of the smooth substrate surface.

Immediately below zone 1 is a sharp boundary to give zone 2, consisting of a recrystallized copper region and a fine crystalline region (Fig. 10c). The former region has a grain size over a wide range from 0.7 to 4 to 5 μm and extends to a depth of 1 to 5 μm, but the usual width is about 1.5 to 2 μm. The final crystalline region has a width of about 0.5 μm and the crystal size is 50 to 100 nm. The structural sequence of "recrystallized grains-fine grains" is repeated 3 to 4 times to give a total depth below the interface of 5 to 8 μm. The structure of zone 2 in consistent with the results of calculations.[5] They indicate that at a depth of 5 to 10 μm below the interface between the coating and the grit-blasted substrate, temperatures within the range 925 to 700 °C are maintained for about 40 μs. Such temperatures would seem to be sufficient to give the partial recrystallization observed in the heavily cold-worked region.

Zone 3 is below zone 2 and consists of recrystallized copper and extends to a depth of 30 to 40 μm below the interface. The modeling studies show that at this depth from the interface, the maximum temperatures attained are about 550 to 600 °C, which is sufficient to produce the observed effects.

Zone 4 of the microstructure is identical to the original susbstrate structure as confirmed by the results of the modeling of the substrate thermal history.[5] Thus, the theoretical results agree well with the experimental data.

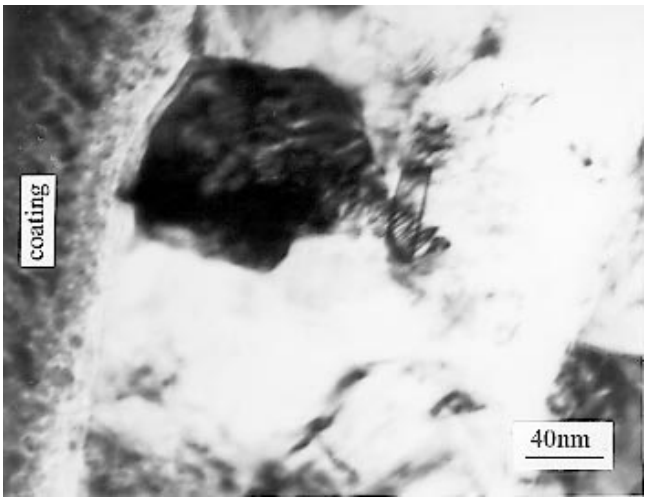

(a)

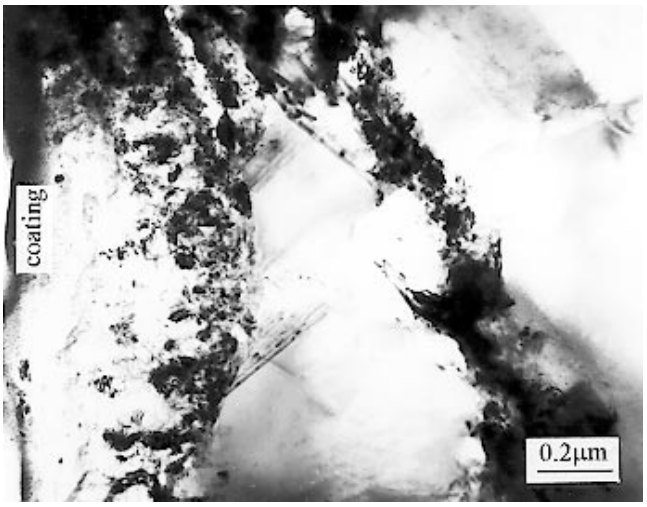

(b)

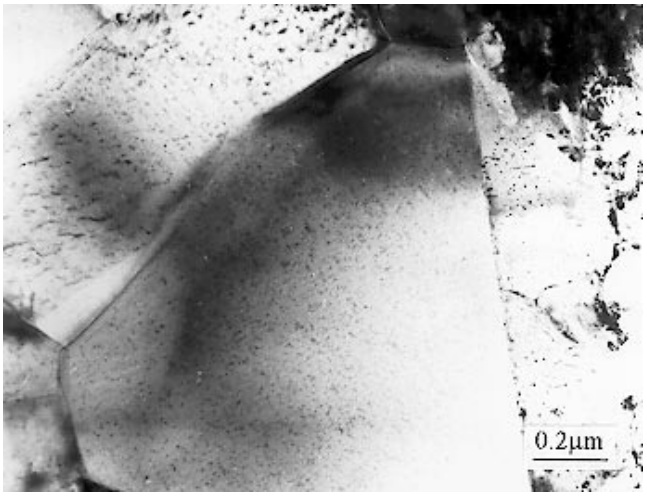

(c)

Fig. 10 Transmission electron micrographs of zone (**a**) 1 of the smooth copper substrate and (**b**) 1 and (**c**) 2 of the grit-blasted copper substrate.

7. Conclusions

Parameters of solidification

- When the first coating layer begins to cool and its solidification starts, the mean solidification velocity varies nonuniformly with the increasing initial temperatures of substrate and coating for both smooth and grit-blasted substrate surfaces.
- The mean thermal gradients G_{S2} at the solidus increase as the substrate initial temperature increases in the case of the smooth substrate surface. These gradients decrease with an increase in substrate initial temperature for the grit-blasted surface. The value of G_{S2} increases when the initial layer temperature is increased, but the behavior of G_{S2} is less uniform in the case of the smooth surface.
- The mean cooling velocities at the solidus increase as the initial layer temperature increases and exhibit the nonuniform behavior with respect to the substrate initial temperature. Mean values of solidification velocity, thermal gradient, and cooling velocity decrease with an increase in layer thickness.

Parameters of the crystalline structure

- In the first and subsequent layers of the coating, both amorphous and fine crystalline structures can be formed because of the very high cooling velocities. The mean values of crystal size ξ for the smooth substrate surface vary nonuniformly with an increase in T_{10} and they decrease as T_{20} increases. In the case of the grit-blasted surface, the mean values of ξ exhibit the nonuniform behavior with respect to T_{10} and T_{20}. The mean values of intercrystalline distance η vary nonuniformly with an increase in T_{10} and T_{20}, for both the smooth and grit-blasted surfaces. An increase in layer thickness causes an increase in the mean values of ξ and η.
- The finest crystalline structure in the case of the smooth substrate surface can be expected when T_{10} = 70 to 120 °C, T_{20} = 1495 to 1500 °C, and δ = 5 to l0 μm. In the case of the grit-blasted surface, the finest crystalline structure is likely to occur when T_{10} = 20 to 50 °C and T_{20} = 1495 °C. The densest crystalline structure for the smooth substrate surface is likely to be formed when T_{10} = 120 °C, T_{20} = 1495 to 1500 °C, and δ = 5 to 10 μm. For the grit-blasted surface, the densest structure seems to be developed when T_{10} = 20 to 50 °C and T_{20} = 1495 °C.
- The finest and densest crystalline structure in the substrate interfacial region in the case of the smooth substrate surface is expected to occur when T_{10} = 20 to 50 °C and T_{20} = 1482 to 1485 °C. In the case of the grit-blasted surface, this structure is likely to be present when T_{10} = 90 to 100 °C, T_{20} = 1490 °C, and δ = 5 to 10 μm.

Structural changes in the substrate solid phase

- During coating formation, some structural changes in the substrate solid state occur because of heating and rapid cooling. Near the substrate-coating interface in the case of the grit-blasted substrate, structural characteristics similar to those formed in melting and rapid solidification of copper occur. The heat transfer from the first coating layer produces recrystallization and recovery to a depth of about 40 μm for the grit-blasted substrate surface. In the case of the smooth surface copper, recrystallization does not occur below the melted zone.

Substrate-coating adhesion

- Substrate-coating mechanical and thermal interactions influence significantly the development of the substrate-coating adhesion during thermal spraying. The generation of groat pressures upon the droplet impact and the substrate roughness enable keying, which is usually assumed to be developed between the coating and the substrate. Substrate-coating thermal interaction leads to partial or complete melting in the substrate interfacial region, and this melted region can then bond readily to the coating. In the case of the grit-blasted substrate surface, the size of the melted region is larger than that for the smooth surface. As a result, the substrate roughness allows more time for good bonding to develop and more strongly adherent coatings to obtain.

Theoretical results agree well with the experimental data available.

Acknowledgments

The authors thank the Generalitat de Catalunya (Project No. SGR 97-15) and CICYT (Project No. MAT 96-0426) for financial support.

References

1. R. McPherson: *Thin Solid Films,* 1981, vol. 83, pp. 297-310.
2. L. Pawlowski: *Science and Engineering of Thermal Spray Coatings,* John Wiley & Sons, New York, NY, 1994, p.p 210-326.
3. R.C. Dykhuizen: *J. Thermal Spray Technol.,* 1994, vol. 3 (4), pp. 351-64.
4. C. Moreau, P. Gougeon, and M. Lamontagne: *J. Thermal Spray Technol.,* 1995, vol. 4, pp. 25-33.
5. V.V. Sobolev, J.M. Guilemany, and J.A. Calero: *J. Mater. Processing Technol.,* 1999, vol. 96, pp. 1-8.
6. V.V. Sobolev, J.M. Guilemany, J. Nutting, and J.R. Miguel: *Int. Mater. Rev.,* 1997, vol. 42 (3), pp. 117-36.
7. V.V. Sobolev, J.M. Guilemany, and J.A. Calero: *Mater. Sci. Technol.,* 1995, vol. 11 (8), pp. 810-19.
8. H. Fukanuma: *J. Thermal Spray Technol.,* 1994, vol. 3 (1), pp. 33-44.
9. T.W. Clyne and S.C. Gill: *J. Thermal Spray Technol.,* 1996, vol. 5 (4), pp. 401-17.
10. V.V. Sobolev and J.M. Guilemany: *Surf. Coating Technol.,* 1994, vol. 70, pp. 57-68.
11. V.V. Sobolev and J.M. Guilemany: *J. Mater. Processing Technol.,* 1996, vol. 58, pp. 227-32.
12. V.V. Sobolev and J.M. Guilemany: *Mater. Lett.,* 1995, vol. 25, pp. 285-89.
13. J.M. Guilemany, V.V. Sobolev, J. Nutting, Z. Dong, and J.A. Calero: *Scripta Metall. Mater.,* 1994, vol. 31 (7), pp. 915-20.
14. J.M. Guilemany, J. Nutting, Z. Dong, and J.M. de Paco: *Scripta Metall. Mater.,* 1995, vol. 33 (7), pp. 1055-62.
15. J.M. Guilemany, J. Nutting, V.V. Sobolev, Z. Dong, J.M. de Paco, J.A. Calero, and J. Fernandez: *Mater. Sci. Eng. A,* 1997, vol. A232, pp. 119-28.
16. *Amorphous Metallic Alloys,* F.E. Luborsky, ed., Butterworthy, London, 1983, pp. 144-68.
17. W. Kurz and D.J. Fisher: *Fundamentals of Solidification,* Trans Tech. Publications Aedermannsdorf, Switzerland, 1984, pp. 65-97.
18. V.V. Sobolev and J.M. Guilemany: *Mater. Lett.,* 1996, vol. 28, pp. 331-35.
19. V.V. Sobolev, J.M. Guilemany, and A.J. Martin: *J. Thermal Spray Technol.,* 1996, vol. 5 (2), pp. 207-14.